A Theoretical Study of the Reaction Paths for Cobalt Cation + Propane

Dmitri G. Fedorov and Mark S. Gordon*

Department of Chemistry and Ames Laboratory, Iowa State University, Ames, Iowa 50011

Received: September 14, 1999; In Final Form: November 2, 1999

The triplet potential energy surface for the reaction of cobalt cation with propane has been studied along the two main reaction pathways leading to the formation of (i) hydrogen and propene and (ii) methane and ethene. Effective core potentials for all elements have been used for all calculations. The geometries have been optimized at the complete active space self-consistent field (CASSCF) level of theory, and the final energetics have been refined at the multireference second-order perturbation theory (MRMP2) level with polarization function augmented basis sets. Reasonable agreement with the experimental energetics has been obtained, and the predicted mechanism is consistent with the experimentally determined mechanism of Haynes, Fisher, and Armentrout (*J. Phys. Chem.* **1996**, *100*, 18300).

1. Introduction

There has recently been considerable experimental[1−3] and theoretical[4−8] interest in bond activation of alkanes by transition metal cations. Van Koppen et al.[1,2] and Haynes[3] et al. studied the reactions of alkanes with cobalt cation by means of guided ion beam spectroscopy. Their studies determined the experimental values for the binding energies and reaction barriers and established that at thermal energies Co^+ reacts with propane to eliminate H_2 and CH_4 with a branching ratio $Co^+(C_2H_4)$ and $Co^+(C_3H_6)$ of 19:81. Musaev et al.[4] studied the mechanism for the reaction of CH_4 and cobalt cation at the CASSCF and SDCI levels. These species are also present on the energy surface of C_3H_8 and Co^+. Perry et al.[5] studied the reaction of small alkanes with Co^+ at the modified coupled cluster functional (MCPF) level of theory and obtained energies for the initially formed molecular complexes of alkanes with Co^+. Holthausen et al. studied the reaction of propane[6] with Fe^+ and ethane[7] with Co^+ at the density functional (DFT), B3LYP[9] level of theory and obtained theoretical predictions for the binding energies and reaction barriers for these systems. Hendrickx et al.[8] studied the stability of hydridoalkyl complexes including C_3H_8 and Co^+ at CASSCF and CASPT2 levels of theory. However, none of the previous computational studies systematically analyzed the ground state potential energy surface for the reactions of Co^+ with propane. The chemical reactions and processes underlying these reactions can be used as models for understanding the mechanisms of the catalytic effect of transition metals on cleavage of bonds in alkanes.

The present work employs multireference second-order perturbation theory to analyze the mechanism for the reaction of Co^+ with propane on the triplet ground electronic state potential energy surface. This includes a comparison of the most likely competing pathways, Co^+ attack on primary or secondary C−H bonds or on a C−C bond, and the competition between production of H_2 and CH_4.

2. Calculation Methods

The search for the transition states and minima on the triplet potential energy surface was conducted with the SBKJ effective core potential (ECP) and the SBKJ basis set,[10] which retains the following orbitals:

$$\text{Co: } 3s^2 3p^6 4s^2 3d^7$$

$$\text{C: } 2s^2 2p^2$$

$$\text{H: } 1s$$

After the geometry optimization at the complete active space (CAS) level, the final energetics were obtained with multireference second-order perturbation theory (MRMP2) and an enhanced basis set labeled SBK*, which contains the following diffuse and polarization functions in addition to the standard SBK basis set:

$$\text{H: s } (\alpha = 0.075)$$

$$\text{C: s } (\alpha = 0.023), \text{ p } (\alpha = 0.021), \text{ d } (\alpha = 0.75)$$

$$\text{Co: d } (\alpha = 0.1219), \text{ f } (\alpha = 1.5)$$

All calculations were performed in C_1 symmetry. In choosing the polarization functions we followed Musaev et al.[4] with the exception of having to reduce the basis set by one set of d functions on C and p functions on H. All exponents are taken from ref 11.

Two other spin multiplicities (singlet and quintet) were probed as well. The singlet surface lies systematically higher than the triplet at all levels of theory; the quintet CASSCF surface lies mostly below the triplet surface, however, the triplet MRMP2 surface is lower than the quintet one. Therefore, the remainder of this work focuses on the triplet state.

The active space used always includes a baseline of eight electrons and six orbitals from $4s^2 3d^6$ or $3d^8$ on Co^+. In addition, the bonds actively involved in the geometry change along each path are included in the pairs of bonding/antibonding orbitals. In general, the first transition state along the reaction path involves breaking one bond, thus the first stage transition states, reactants, and intermediates each requires 10 electrons in 8 orbitals [10/8]. In some cases a neighbor C−H bond is found to be very close to the cobalt and thus influential upon the system; in this case [12/10] active space is used. For intermediates, the [10/8] active space is often sufficient. For the second stage transition states generally a σ and a π bond are formed,

10.1021/jp9932766 CCC: $19.00
Published on Web 12/28/1999

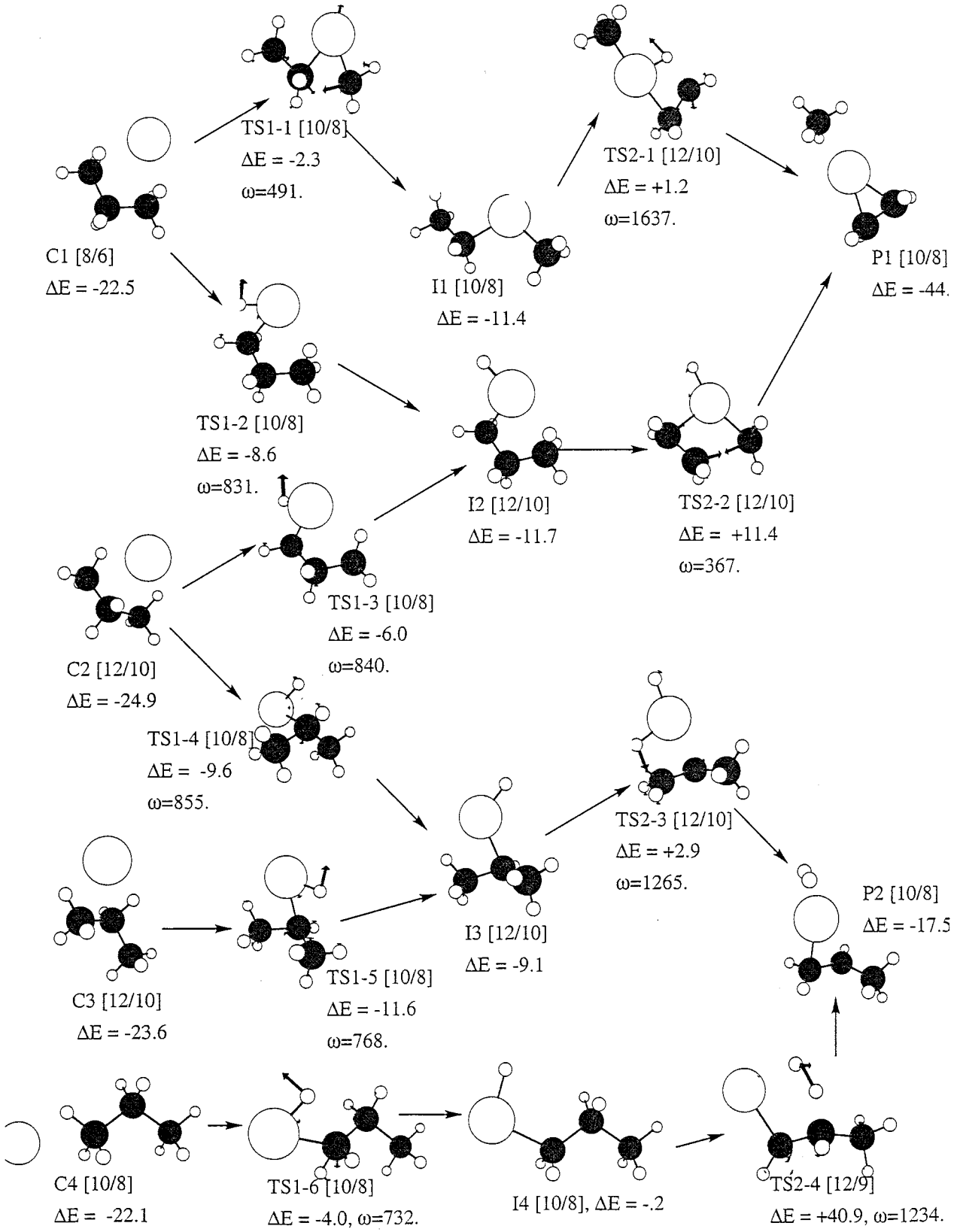

Figure 1. The energy extrema on the investigated part of the reaction surface. Each extremum features a label, CAS active space [*m*/*n*], *m* electrons in *n* orbitals, and energy (Δ*E*, in kcal/mol) relative to $Co^+ + C_3H_8$ at infinite distance at MRMP2 level of theory. In addition, arrows on transition state structures show the direction of the imaginary mode and the imaginary frequency ω is given in cm^{-1}.

thus such transition states require a [12/10] active space. The products are calculated by correlating the π bond and are thus done using the [10/8] active space.

For transition metal complexes, there is no computationally feasible active space that can be consistently used throughout all calculations on a potential energy surface. Therefore, the general expectation is that the subsequent MRMP2 calculation makes up for the different active spaces used at different points on a potential energy surface. Since the MCSCF wave function accounts for the near degeneracies, while the MRMP2 accounts

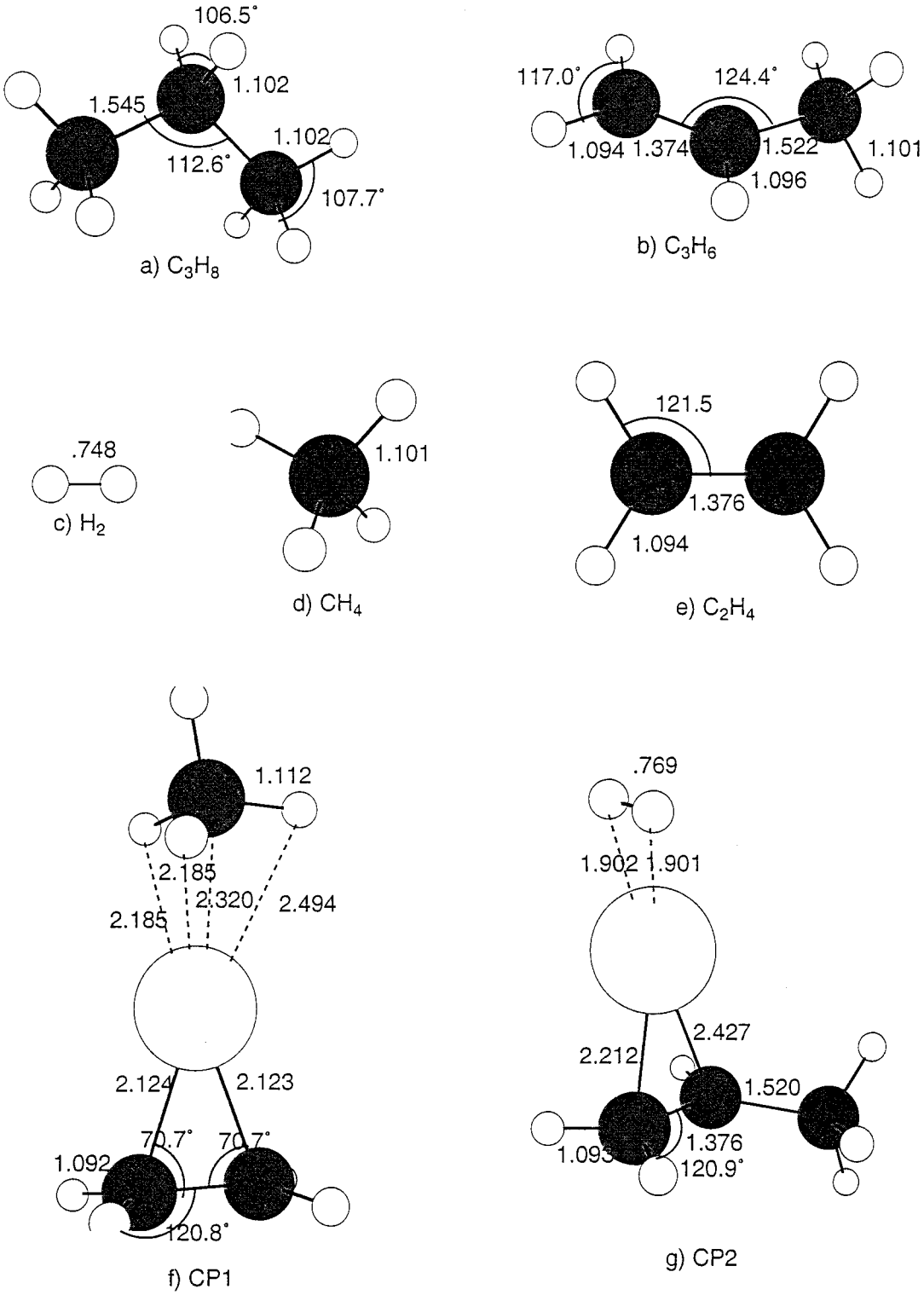

Figure 2. Structures of the reactants and products. The distances are in Å and the angles are in degrees.

for dynamic correlation, this is a reasonable approach. Indeed, several tests suggest that the errors introduced by this approach are only on the order of 2−5 kcal/mol. Some of the active spaces listed above may become inadequate during an IRC run. An example is the formation of the CP1 product discussed below. In this case, the active space used for describing the transition states leading to it is [12/10], with only one C−H bond of the forming CH_4 molecule included. However, three C−H bonds facing Co^+ are nearly equivalent. Thus, ideally one may wish to correlate all three C−H bonds, but this would result in a nearly intractable [16/14] active space.

Another problem that may be encountered in choosing an active space lies in the orbitals. The antibonding C−H orbitals are often lower in energy than the excited 4s4p orbitals on Co^+. It is found that the competition between excited 4s4p orbitals and the antibonding orbitals results in the unwanted penetration of the 4s4p Co orbitals into the active space, especially when there are two antibonding orbitals (i.e., with the [12/10] active space). This penetration lowers the CAS energy but raises the MRMP2 energy. Sometimes a good choice of starting orbitals helps keep the penetration from occurring. In other cases when this does not work, the freezing of the chemical core during

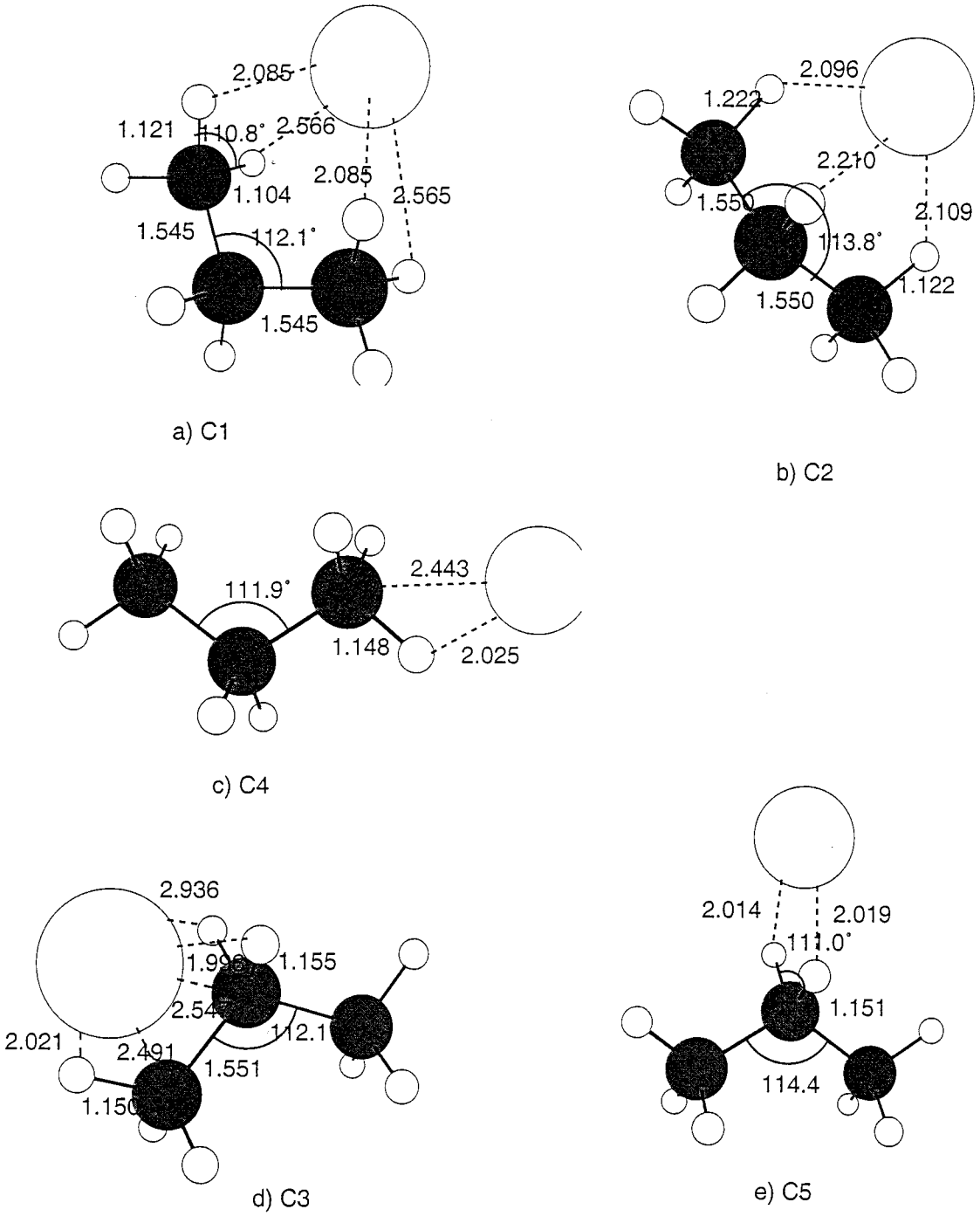

Figure 3. Addition complexes. The distances are in Å and the angles are in degrees.

the CAS step is found to help reduce admixing of the unwanted excited orbitals on cobalt.

For the MRMP2 calculations it is found that correlation of the core 3s3p orbitals on Co incorrectly predicts the splitting between the atomic triplet and quintet levels whereas not correlating these orbitals reproduces the splitting reasonably. All MRMP2 calculations thus do not correlate these orbitals.

For all calculations the quantum chemistry code GAMESS[12] has been used.

3. Results and Discussion

A. Overview. An overview of the triplet potential energy surface is presented in Figure 1, with the geometries of reactants and products given in Figure 2. Each reaction path generally proceeds from the formation of the initial complexes (see structures C1−C5 in Figure 3) of the cation with the neutral alkane molecule bound by electrostatic attraction. Then an intermediate (structures I1−I4 in Figure 5) is formed via a first stage insertion transition state (structures TS1-1 to TS1-6 in Figure 4). One initial complex C5 is found to lead to high energy cationic products through a high barrier transition state, so it was not pursued further. The intermediates proceed to the products via the second stage transition states (structures TS2-1 to TS2-4 in Figure 6). Overall, the reaction scheme agrees with the one proposed by Haynes et al.,[3] although experimentally it was not possible to distinguish between several complexes or transition states leading to the same product. Some of the six pathways were found to merge to form four major reaction paths.

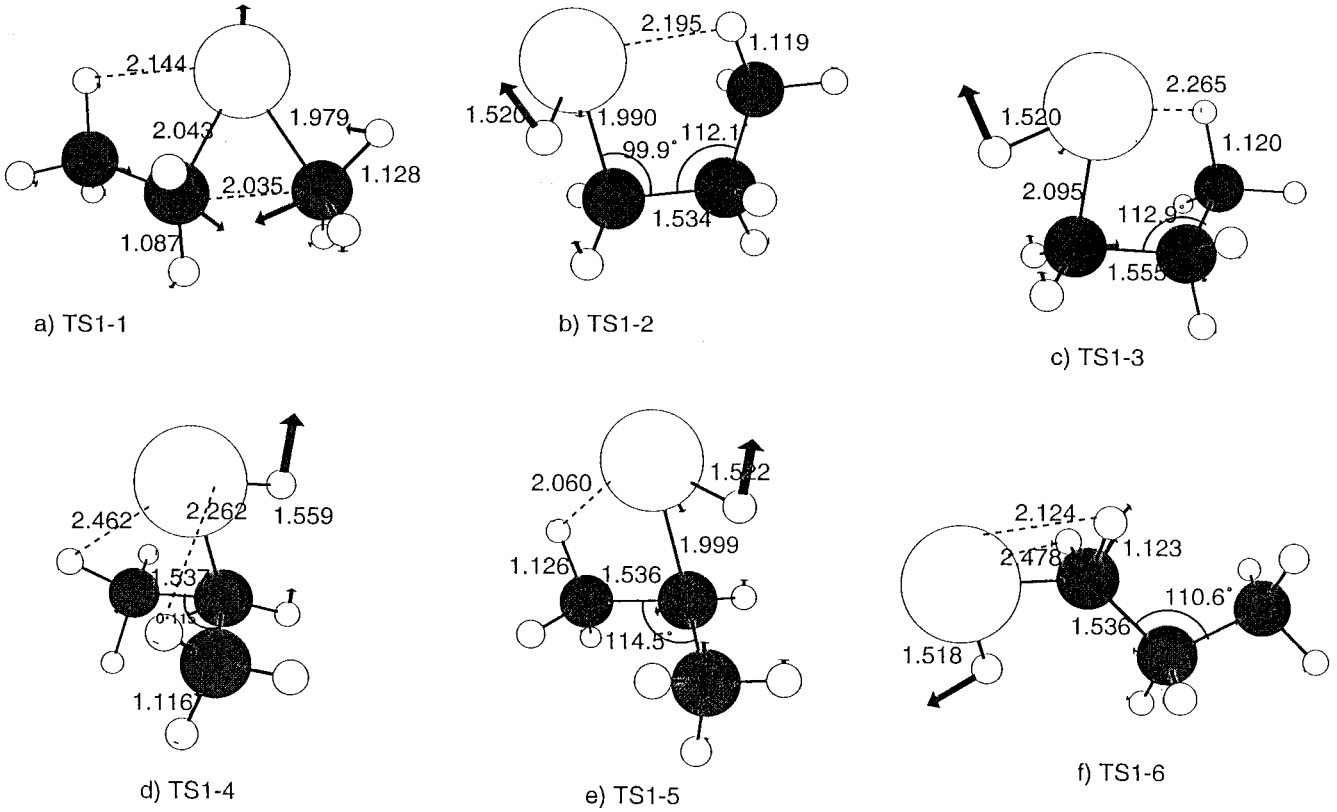

Figure 4. The first stage transition states. The distances are in Å and the angles are in degrees. The direction of the imaginary mode is shown with arrows.

Of these four, two (see Figure 1) are found to have significantly higher barriers so that only one pathway from the reactants to products is energetically accessible for each product. Note that all structures along these paths were determined at the CASSCF level of theory, whereas MRMP2 relative energies (MRMP2//CASSCF) are given in Figure 1 and Table 1. This explains why some transition states are lower in energy than connecting local minima at the higher level of theory.

The results are summarized in Table 1. The comparison with the results obtained by other researchers is given in Table 2. These data are discussed in more detail below.

B. Reactants and Products. The optimized geometries for the reactants and products are presented in Figure 2.

Alkanes (CH_4, C_3H_8) and H_2 are formed with σ-bonds only and therefore were optimized at the RHF level of theory, whereas alkenes (C_2H_4,C_3H_6) were optimized at the [2/2] CAS level. In Table 2, R1 denotes $C_3H_8+Co^+$, P1 denotes $CH_4+C_2H_4+Co^+$, and P2 denotes $H_2+C_3H_6+Co^+$, where the + sign implies infinite separation between the species. In contrast, CP1 and CP2 denote molecular complexes at close distances.

C. Initial Complexes. The geometrical parameters for the complexes are given in Figure 3. The energies of all five complexes relative to separated reactants are quite similar and lie in the range of −22.1 to −26.1 kcal/mol, somewhat below the experimental value of −30.9 kcal/mol.[2]

The difference in energy between the five complexes C1−C5 is explained by the extent to which Co^+ is able to approach the nucleophilic σ bonds in C_3H_8. It appears that Co^+ is capable of interacting with at most two H atoms, indicated by Co−H distances of about 2 Å, with the exception of C2. The binding energy of C4 (one bound H atom) is somewhat smaller (22.1 kcal/mol) than that of the other four complexes. If more than two H atoms are present in the vicinity of Co^+, the binding energy is lowered due to repulsion; this is evident in C1 and C3 with two extra H atoms repelling Co. Thus, the two complexes C2 and C5 are the lowest in energy; in the case of C2, one extra H is present. Interestingly, even though the binding energy is the largest in the case of no repelling H atoms (C5), the subsequent points along this reaction path are high in energy. This is apparently due to the absence of stabilizing electrostatic interactions (e.g., C−H or C−C with Co^+) to balance the energy required to break bonds in the presence of Co^+. The H atoms which interact with Co^+ have the corresponding C−H distances lengthened by about 0.02−0.05 Å.

For both α and β C−H insertion, the distance between Co and the detached H atom is about 1.5 Å in the first stage transition states and 1.6 Å in the intermediates. In the second stage transition states (Figure 6) the Co−H distance varies considerably depending upon the nature of the transition state. The distance between Co and C from which a hydrogen or carbon atom is detached is about 2 Å.

D. CH_4 Elimination. The CH_4 elimination path begins from the molecular complexes C1 and C2 via three transition states: TS1-1 (C−C insertion), TS1 2 (α C−H insertion), and TS1-3 (α C−H insertion), see Figure 4. The two α C−H insertion transition states are similar in energy (−8.6 and −6.0 kcal/mol) and geometry and correspond to two different positions from which Co^+ attacks a C−H bond. The reaction path for these transition states merges into an intermediate I2, whereas the C−C insertion proceeds independently to form the intermediate I1 (see Figures 1 and 5). Subsequently, the reaction paths leading from I1 and I2 converge to the product P1 via transition states TS2-1 and TS2-2, shown in Figure 6. The α C−H insertion path, however, shows a significantly higher reaction barrier compared to the C−C insertion (+11.4 vs +1.2 kcal/mol). Therefore, we conclude that the CH_4 elimination occurs with a +1.2 kcal/mol barrier through a C−C insertion transition state. The resulting complex of Co^+, CH_4, and C_2H_4 is predicted to

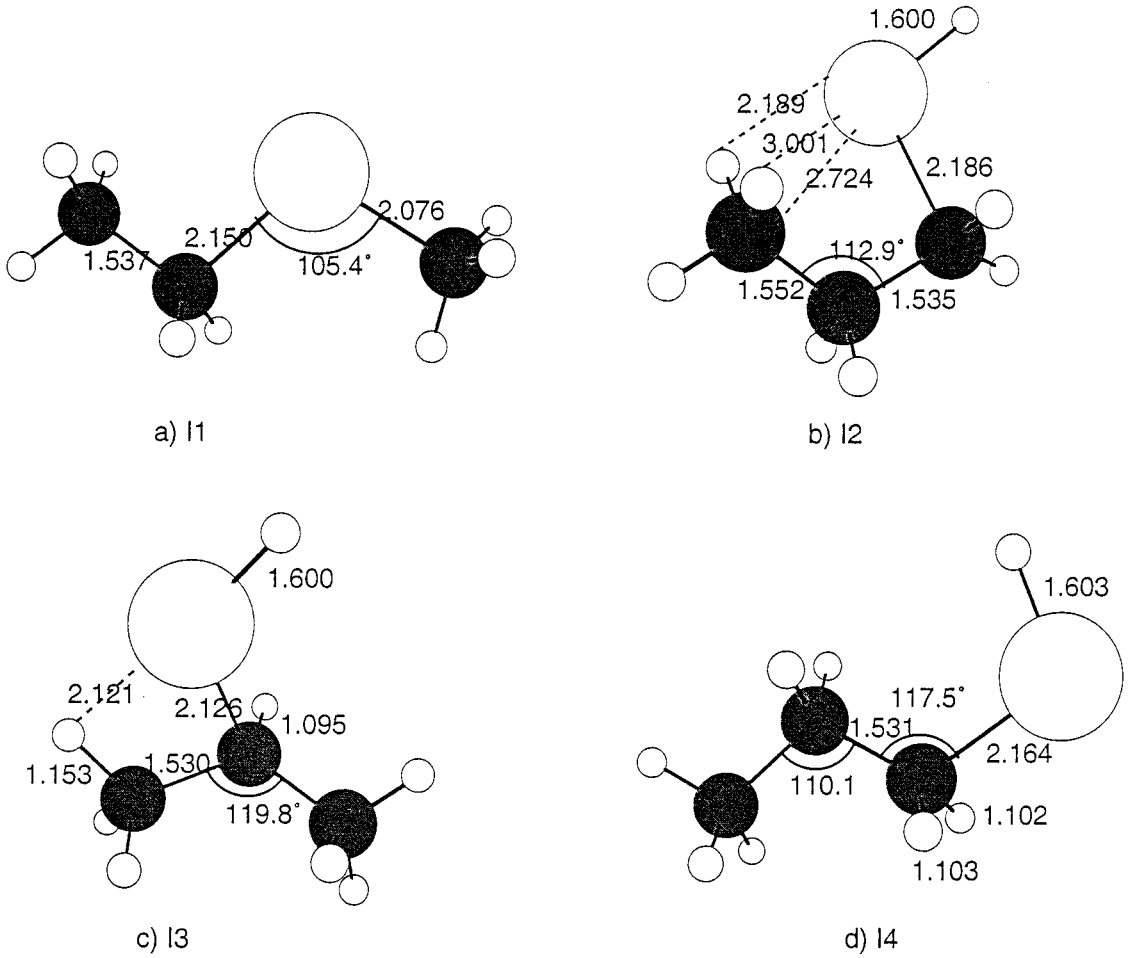

Figure 5. The intermediates. The distances are in Å and the angles are in degrees.

TABLE 1: MRMP2 Relative Energies for the Points along the Path

compd	SBK, kcal/mol	ZPE, kcal/mol	SBK*, kcal/mol	SBK*+ZPE
R1	0	0	0	0
C1	−28.4	+0.3	−22.8	−22.5
C2	−23.9	+0.1	−25.0	−24.9
C3	−24.7	−0.8	−22.8	−23.6
C4	−19.4	−0.3	−21.8	−22.1
C5	−25.5	−0.8	−25.3	−26.1
TS1−1	+2.8	−1.9	−0.4	−2.3
TS1−2	−0.7	−3.8	−4.8	−8.6
TS1−3	+1.6	−3.7	−2.3	−6.0
TS1−4	−7.8	−3.8	−5.7	−9.6
TS1−5	−3.6	−3.8	−7.8	−11.6
TS1−6	+3.2	−3.9	−0.1	−4.0
I1	−9.4	−3.4	−8.0	−11.4
I2	−4.6	−4.7	−7.0	−11.7
I3	−2.4	−5.5	−2.6	−9.1
I4	+5.8	−4.7	+4.5	−0.2
TS2−1	+8.3	−6.4	+7.6	+1.2
TS2−2	+16.0	−6.4	+17.8	+11.4
TS2−3	+6.8	−8.8	+11.7	+2.9
TS2−4	+44.2	−8.0	+48.9	+40.9
CP1	−38.9	−3.0	−41.5	−44.5
CP2	−6.9	−5.8	−11.7	−17.5
P1	+18.6	−6.1	+25.7	+19.6
P2	+29.7	−9.9	+34.8	+24.9

have a 44.5 kcal/mol binding energy. The corresponding product complex CP1 has Co^+ bound to two hydrogen atoms in CH_4 and to the π bond on C_2H_4. The Co−H distance is larger by about 0.2 Å compared to the case of $C_3H_8 + Co^+$; it is likely that this is due to repulsion from the π electron density.

TABLE 2: Comparison to Other Available Data, kcal/mol, Relative to $Co^+ + C_3H_8$

compd	this work	Perry et al.[5]	Haynes et al.[3]	Barrow[14]
C1, η^4	−22.5	−27.6	−30.9	
C2	−24.9			
C3	−23.6			
C4, η^2	−22.1	−26.8		
C5, η^3	−26.1			
TS1-1	−2.3		−1.8	
TS1-2	−8.6		−10.6	
TS1-3	−6.0			
TS1-4	−9.6			
TS1-5	−11.6			
TS1-6	−4.0			
I1, **3**	−11.4		−4.6	
I2, **2**	−11.7		−10.6	
I4, **2**	−0.2			
I3, **1**	−9.1			
TS2-1, **9**	+1.2		+1.2	
TS2-2, **8**	+11.4			
TS2-3, **6**	+2.9		−6.7	
TS2-4, **7**	+40.9			
CP1	−44.5		"−39"[a]	
CP2	−17.5		"−31"	
P1	+19.6			+18.0
P2	+24.9			+28.0

[a] We could not clearly identify what the exact energies are from ref 2. The values in quotes have been deduced from Figure 8 of that paper and may not be accurate.

E. H_2 Elimination. The H_2 elimination path is topologically similar to that of the CH_4 elimination. The α C−H insertion forms an independent path through the transition state TS1-6

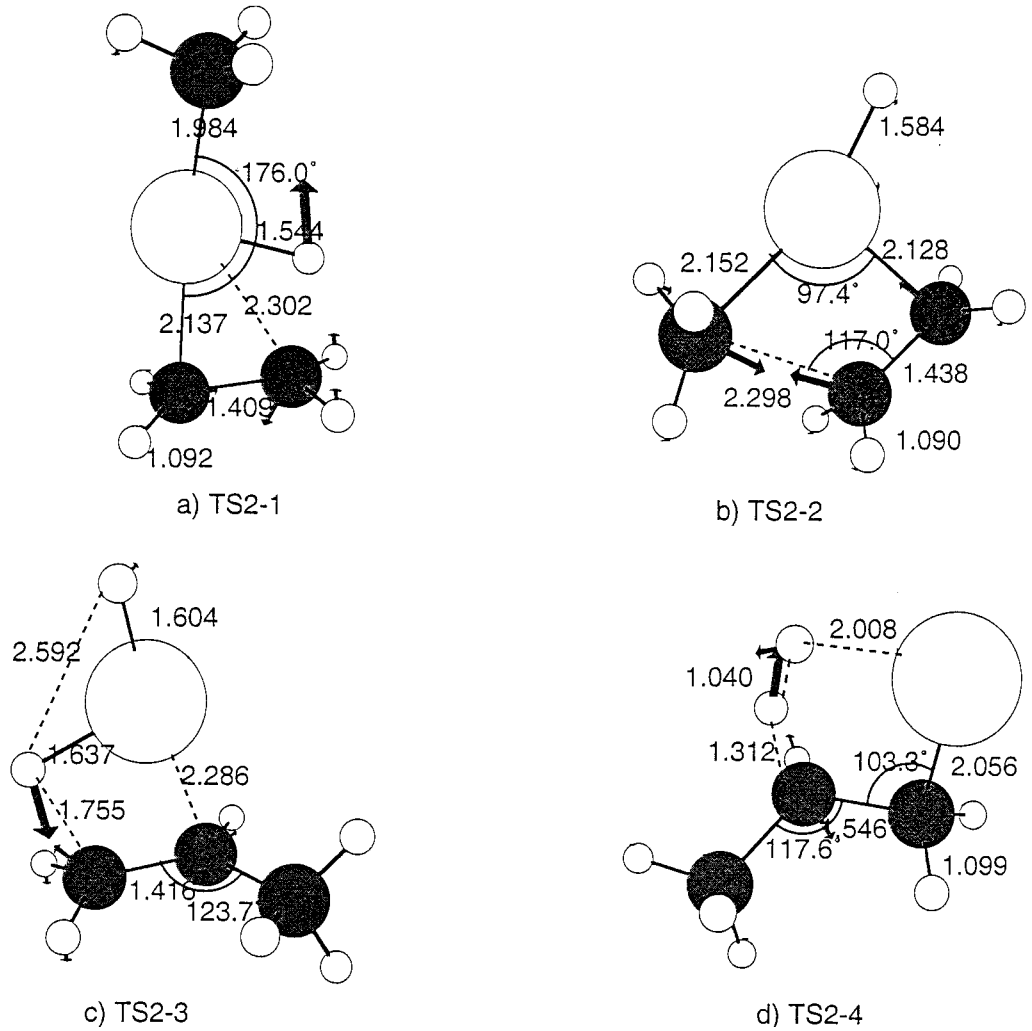

Figure 6. The second stage transition states. The distances are in Å and the angles are in degrees. The direction of the imaginary mode is shown with arrows.

to the intermediate I4, whereas β C−H insertion occurs at two different positions from which the Co^+ attacks a C−H bond. The two β C−H insertion transition states TS1-4 and TS1-5 are similar in energy (−9.6 and −11.6 kcal/mol) and in geometry. They converge to the intermediate I3. The reaction barrier for the final transition state is much larger for the α C−H path (TS2-4) as compared to the β C−H insertion path (TS2-3) (+40.9 vs +2.9 kcal/mol). Thus, we conclude that H_2 elimination occurs via the β C−H insertion with a +2.9 kcal/mol barrier. The products H_2 + C_3H_6 (propene) form a molecular complex with Co^+ with 17.5 kcal/mol binding energy. The resultant complex CP2 appears to be asymmetric with respect to the π bond on C_3H_6: Co^+ prefers to be closer to the terminal C atom. The distance to the hydrogen molecule is quite large, 1.861 Å, so that one can conclude that most of the binding occurs to the π bond on C_3H_6 in contrast to CP1 where the binding involves σ bonds as well. The latter is reflected in the larger binding energy of CP1 as compared to CP2 (44.5 vs 15.5 kcal/mol).

Conclusions

The predicted mechanism appears to be quite consistent with that proposed by Haynes, Fisher, and Armentrout. The CH_4 elimination is predicted to occur with a +1.2 kcal/mol barrier through a C−C insertion transition state, while H_2 elimination occurs via a β C−H insertion with a +2.9 kcal/mol barrier. Overall, the energetics predicted in this work appear to be largely in good agreement with experiment,[3] although some discrepancies are observed. Some of the experimental energetics quoted in Table 2 were deduced from figures in that paper, and therefore may not be accurate. Based on the comparison in Table 2, the errors in the calculations range from 1 to 8 kcal/mol (omitting the experimental values in quotes). So, the average error in the present results is estimated to be on the order of 5 kcal/mol. So, it is likely that the qualitative conclusions drawn here are reliable. Most computational errors are attributed to the inaccuracies and approximations in the calculations, among which the basis set size and the use of ECPs are considered to be the major factors. Nevertheless, overall the theoretical prediction that the reaction should proceed at room temperature agrees with experiment.[3]

The results obtained by Perry et al.[5] appear to be in better agreement with the experiment than ours for the predicted binding energies of the initial complexes (the only part of the surface they examined). This may be attributed, at least in part, to their use of a better basis set. The results by Hendrickx[8] et al. appear to disagree with both our results and experiment, predicting high barriers on the order of 8.2 and 9.6 kcal/mol for the primary and secondary insertion and high energetics for the intermediate as well, 8.0 and 13.4, correspondingly. This

disagreement is surprising, as their method of calculation, CASSCF augmented by CASPT2, is quite similar to our approach.

Acknowledgment. This work was supported by the Ames Laboratory via a grant from the Basic Energy Sciences Division of the Department of Energy. Discussions with Dr. Michael Schmidt, Dr. Jerzy Moc, and Dr. Jamal Musaev are gratefully acknowledged.

References and Notes

(1) van Koppen, P. A. M.; Brodbelt-Lustig, J.; Bowers, M. T.; Dearden, D. V.; Beauchamp, J. L.; Fischer, E. R.; Armentrout, P. B. *J. Am. Chem. Soc.* **1990**, *112*, 5663.

(2) van Koppen, P. A. M.; Brodbelt-Lustig, J.; Bowers, M. T.; Dearden, D. V.; Beauchamp, J. L.; Fischer, E. R.; Armentrout, P. B. *J. Am. Chem. Soc.* **1991**, *113*, 2359.

(3) Haynes, C. L.; Fisher, E. R.; Armentrout, P. B. *J. Phys. Chem.* **1996**, *100*, 18300.

(4) Musaev, D. G.; Morokuma, K.; Koga, N.; Ngyuen, K. A.; Gordon, M. S.; Cundari, T. R. *J. Phys. Chem.* **1993**, *97*, 11435.

(5) Perry, J. K.; Ohanessian, G.; Goddard, W. A., III *J. Phys. Chem.* **1993**, *97*, 5238.

(6) Holthausen, M. C.; Koch, W. *Helv. Chim. Acta* **1996**, *79*, 1939.

(7) Holthausen, M. C.; Koch, W. *J. Am. Chem. Soc.* **1996**, *118*, 9932.

(8) Hendrickx, M.; Ceulemans, M.; Vanquikenborne, L. *Chem. Phys. Lett.* **1996**, *257*, 8.

(9) Becke, A. D. *Phys. Rev. A* **1988**, *38*, 3098. Becke, A. D. *J. Chem. Phys.* **1993**, *98*, 1372. Becke, A. D. *J. Chem. Phys.* **1993**, *98*, 5648. Lee, C.; Yang, W.; Parr, R. G. *Phys. Rev. B* **1988**, *37*, 785.

(10) Stevens, W. J.; Krauss, M.; Basch, H.; Jasien, P. G. *Can. J. Chem.* **1992**, *70*, 612.

(11) Dunning, T. H., Jr.; Hay, P. J. *The Methods of Electronic Structure Theory*; Schaefer, H., III, Ed.; Plenum: New York, 1977.

(12) Schmidt, M. W.; Baldridge, K. K.; Boatz, J. A.; Elbert, S. T.; Gordon, M. S.; Jensen, J. H.; Koseki, S.; Matsunaga, N.; Nguyen, K. A.; Su, S. J.; Windus, T. L.; Dupuis, M.; Montgomery, J. A. *J. Comput. Chem.* **1993**, *14*, 1347.

(13) Glaesemann, K. R.; Gordon, M. S.; Nakano, H. *PCCP Phys. Chem. Chem. Phys.* **1999**, *1*, 967.

(14) Barrow, G. M. *Physical Chemistry*; McGraw-Hill: New York, 1979.